3B2v8.06a/w (Dec 5 2003).51c + model | JQSR : 1807 | Prod.Type:FTP pp.1–12(col.fig.:NIL) | ED:AjithG.P. PAGN:Jay SCAN:

ARTICLE IN PRESS

ELSEVIER

Quaternary Science Reviews ▮ (▮▮▮▮) ▮▮▮–▮▮▮

QSR

A stalagmite record of changes in atmospheric circulation and soil processes in the Brazilian subtropics during the Late Pleistocene

Francisco W. Cruz Jr.[a,b,*], Stephen J. Burns[a], Ivo Karmann[b], Warren D. Sharp[c], Mathias Vuille[a], José A. Ferrari[d]

[a]*Department of Geosciences, Morrill Science Center, University of Massachusetts, Amherst, MA 01003 USA, 01003*
[b]*Instituto de Geociências, Universidade de São Paulo, Rua do Lago, 562, 05508-080, São Paulo-SP, Brazil*
[c]*Berkeley Geochronology Center, 2455 Ridge Road, Berkeley, CA 94709, USA*
[d]*Instituto Geológico-SMA, Av. Miguel Stefano 3900, 04301-903, São Paulo, Brazil*

Received 7 October 2005; accepted 21 February 2006

Abstract

We present a high-resolution, 116,000-year carbon stable isotope record from a stalagmite from southern Brazil, which has been precisely dated using the U-series method. Evaluation of carbon and oxygen isotope ratios together with the speleothem growth history suggest that the carbon isotopic composition of the speleothem is primarily controlled by biogenic CO_2 supply from the soil, which is in turn affected by temperature and secondarily rainfall amount. Thus, the speleothem provides evidence of paleoenvironmental change in southern Brazil during the last glacial period. Predominantly high $\delta^{13}C$ values and low stalagmite growth rates reflect persistent cool conditions during most of the glacial period in subtropical Brazil. This cooling is probably related to an intensified extratropical circulation with more frequent and intense cold surges, reaching a maximum at approximately 19 ky B.P. This cooling tendency is interrupted during periods of high obliquity values within the full glacial period at 93–85 and 47–40 ky B.P, and after 19 ky B.P, when a dramatic decrease in $\delta^{13}C$ marks the deglaciation time in the continent. Unlike $\delta^{18}O$, the $\delta^{13}C$ record does not exhibit a strong response to precessional forcing; instead it shows a strong 40 ky obliquity signal. Here we propose that local temperature and thus the biological processes in the soil are primarily steered by the gradients of temperature between low and mid-high latitudes, which influence the meridional heat transport. These gradient changes in turn are paced by obliquity.

1. Introduction

Secondary carbonates precipitated in caves, termed speleothems, are potential records of paleoenvironmental response to changes in atmospheric circulation because the climate signal embedded in stable oxygen isotopes of speleothems, $\delta^{18}O$, is primarily controlled by rainfall isotopic composition (Gascoyne, 1992; McDermott, 2004). Time series of $\delta^{18}O$ can then be combined with other proxies of processes occurring in soil such as carbon stable isotopes, $\delta^{13}C$, (Dorale et al., 1998; Genty et al., 2003), trace elements (Baldini et al., 2002), speleothem growth-rates (Baker et al., 1998; Polyak et al., 2004) and organic matter fluorescence properties (Charman et al., 2001). A multi-proxy study from the same speleothem thus allows precise determination of relative timing various climate proxies held in a single archive. The great majority of speleothem-based paleoclimate studies focus on interpreting oxygen isotope time series, with far fewer studies attempting to infer climate variability from carbon isotopes. In part, this hesitancy is surely due to the relative complexity of interpreting $\delta^{13}C$. Nevertheless, changes in the $\delta^{13}C$ values of speleothems should in most cases be the result climate variation. Here, we analyze the unpublished $\delta^{13}C$ data set from stalagmite Bt2 by comparing it with the $\delta^{18}O$ record and growth rates from the same stalagmite (Cruz Jr. et al., 2005a) and other regional records. Our aim is to investigate the effect of changes in large-scale atmospheric circulation on the temperature-driven biolo-

*Corresponding author. Department of Geosciences, Morrill Science Center University of Massachusetts, Amherst, MA 01003, USA. Tel.: +1 413 545 0659; fax: +1 413 545 1200.

0277-3791/$ - see front matter © 2006 Published by Elsevier Ltd.
doi:10.1016/j.quascirev.2006.02.019

gical activity and soil CO_2 productivity during the last glaciation.

Carbon isotope signatures in speleothems are related to the sources of dissolved carbon in the dripwater such as soil CO_2, carbonate bedrock and the atmosphere. Their relative contribution is dependent upon the mechanisms controlling the bedrock dissolution and carbonate precipitation in the cave system (Hendy, 1971; Genty et al., 2001a). The $\delta^{13}C$ of speleothems can be linked to climate-driven vegetation changes because the isotopic composition of soil organic matter (SOM) is influenced by changes in plant communities due to the large differences in the carbon isotopic composition between C_3 ($\delta^{13}C$ from -32 to $-20‰$) and C_4 ($\delta^{13}C$ from -17 to $-9‰$) plants, typically tree and grass species, respectively (Boutton, 1996). This difference allows reconstruction of shifts in vegetation patterns from forests to grasslands as long as comparison with pollens records is possible (Dorale et al., 1998; Denniston et al., 1999; Frumkim et al., 2000). In regions where C_4 plants are rare, however, as for example in Europe (Genty et al., 2001a, 2003), Australia (Desmarchelier et al., 2000) and New Zealand (Williams et al., 2005), other processes must be responsible for driving changes in speleothem $\delta^{13}C$.

One major influence on $\delta^{13}C$ should be the rate of CO_2 production in soil by plant respiration and microbiologically induced organic matter decomposition. Increased soil respiration leads to higher soil P_{CO_2} and consequently more negative $\delta^{13}C$ values of soil CO_2 (Hesterberg and Siegenthaler, 1991; Amundson et al., 1998). The combined effects of precipitation and temperature on CO_2 production and cycling vary in a complex way depending on how the local environment influences the proportion between isotopically depleted, soil organic matter-derived and isotopically enriched, limestone or dolostone carbon sources in speleothems (Genty et al., 2001a; Linge et al., 2001, Baldini et al., 2005). Periods of increased rates of biological soil CO_2 have been linked to warmer conditions in Europe (Genty et al., 2003; Drysdale et al., 2004), wetter conditions in New Zealand (Williams et al., 2005) and El Niño events in Central America (Frappier et al., 2002). Furthermore, co-variation between $\delta^{13}C$ and speleothem growth rates has been associated with the amount of CO_2 available in the soil (Plagnes et al., 2002; Drysdale et al., 2004) because dissolved CO_2 concentration is a major factor affecting bedrock dissolution and Ca^{2+} concentration in seepage waters (Genty et al., 2001b; Kaufmann and Dreybrodt, 2004).

Possible kinetic isotope fractionation effects must, of course, be considered before interpreting carbon isotope records in terms of paleoenvironmental changes, because they can override changes in organic productivity associated with the soil zone (Spötl et al., 2005). Non-equilibrium fractionation may cause enrichment in ^{13}C under evaporative conditions, which is sometimes expressed in ancient stalagmite layers as widely ranging $\delta^{18}O$ and strong linear correlation between $\delta^{18}O$ and $\delta^{13}C$ (Hendy, 1971; Linge et al., 2001). Higher $\delta^{13}C$ values than predicted by isotopic equilibrium equations between calcite speleothems and its parental water can also result from CO_2 degassing during prior calcite precipitation in the unsaturated zone above the cave (Baker et al., 1997). This process is used to explain the increase in Mg concentration from drip solution by preferential removal of Ca in calcite precipitated along the flow path (Fairchild et al., 2000). In addition, the CO_2 degassing can also promote progressive enrichment in $\delta^{13}C$ during calcite precipitation, because lighter carbon is preferentially lost from solution, so that speleothems with lower growth rates might have higher $\delta^{13}C$ (Dulinski and Rozanski, 1990; Genty et al., 2001a). Changes in calcite $\delta^{13}C$ resulting from this process are considered negligible, however, by some authors (Hendy, 1971; Bar-Matthews et al., 1996; Mickler et al., 2004).

CO_2 degassing can be also influenced by shifts in cave atmospheric circulation because it can control the pCO_2 gradient between dripwater and cave atmosphere, as is observed in areas with contrasting seasonal temperatures in Europe (Spötl et al., 2005). Incursions of low pCO_2 air from outside driven by warmer temperatures toward the cave during the winter can significantly drop the cave atmospheric pCO_2 and thereby increase the CO_2 degassing from solution due to higher gradients between dripwater and cave atmosphere. In this way, cave air dynamics can be superimposed on the environmental changes in soils. On the other hand, environmental changes may still be captured in speleothem $\delta^{13}C$ even if it is controlled by degassing, as this mechanism shows a strong dependence on cave outside temperature, so that enriched values can be linked to colder and more persistent winters (Spötl et al., 2005).

2. Study area and modern climatology features

Stalagmite Bt2 was collected from Botuverá cave (27°13′24″S; 49°09′20″W), southern Brazil (Fig. 1a) at the end of the cave's main gallery, approximately 300 m from its only entrance and about 110 m below the surface (Fig. 1b). The sample is a candle-like calcite stalagmite 70 cm tall, which was active at the time of sampling. The cave was developed in low metamorphic grade limestones of the Meso- to Neoproterozoic Brusque Group (Campanha and Sadowski, 1999). The site is located at the transition between the Atlantic coastal plain and the Brazilian highland plateaus at an elevation of 250 m adjacent to Serra Geral (Fig. 1). Dense, tropical Atlantic rainforest and mature, clay-rich soils a few meters thick cover the area.

The present-day climate at the cave site is subtropical humid, with nearly saturated mean relative humidity and rainfall that is uniformly distributed throughout the year (Rao and Hada, 1990). The mean annual precipitation (MAP) for 30 years at a meteorological station located 40 km from Botuverá and at similar altitude was 1500 mm (Source Climerh-Epagri, pers. com.). The external mean annual temperature (MAT) at Botuverá cave between 2000

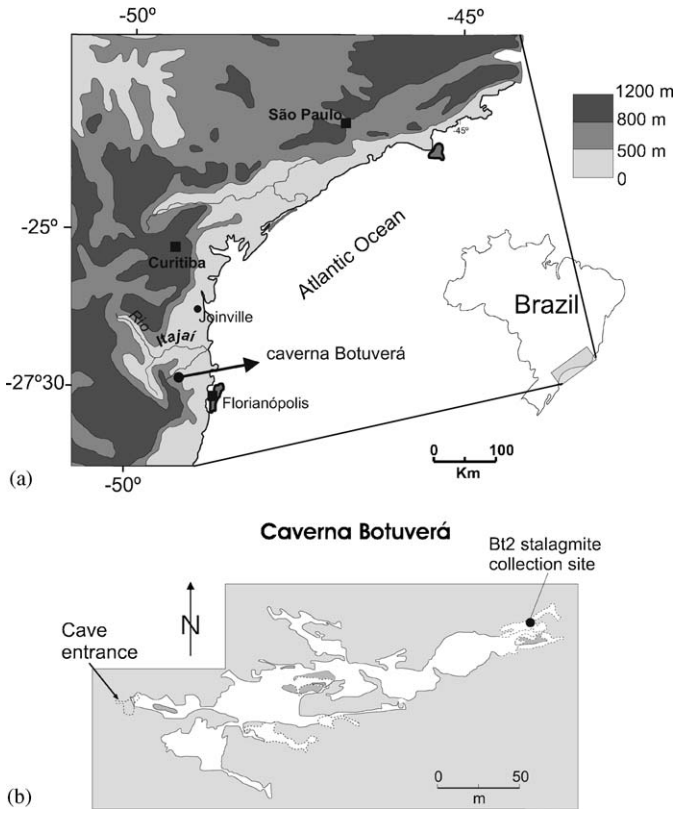

Fig. 1. Location map of the study site in southern Brazil. (a) Botuverá Cave is located at the transition between the Atlantic coastal plain and the Serra Geral plateau. (b) Plan map of cave showing the site of the Bt2 sample collection.

and 2002 was 18.9 °C, in close agreement with internal MATs of 18.6 and 19.0 °C. During the austral winter (June–August), relative cold conditions prevail and mean temperature drops to 13.9 °C near the cave site. The summer mean temperature (December-February) averaged 20.8 °C between 1968 and 1996, based on NCEP/NCAR reanalysis data (derived from grid cell centered at 27.5°S50°W; Kalnay et al., 1996). On average the temperature difference between the warmest and coldest month in the region (February and July) is ~12 °C, but the annual temperature range can vary from ~7 to 25 °C.

The climate of subtropical South America to the east of the Andes is strongly influenced by interactions between the tropical and extratropical circulation and related meridional heat transport. Regional temperature variability is linked to the intensity and frequency of extratropical cold fronts and associated transient incursions of mid-latitude cold and dry air into subtropical and tropical South America, as documented among others in Garreaud (1999, 2000), Seluchi and Marengo (2000), Vera and Vigliarolo (2000), Vera et al. (2002), and Marengo et al. (2002). Southern Brazil is located along a preferred pathway of equator-ward propagating cold-air incursions downstream of the Andes. The upper-tropospheric circulation provides large-scale forcing for cold surge frequency and intensity, predominantly in the form of vorticity advection and thus has a significant impact on the climatological distribution of near-surface temperature.

The most dramatic cold episodes occur during austral winter, favored by stronger meridional temperature gradients between low and mid-latitudes due to colder land and a warmer ocean. The low-level atmospheric circulation associated with extreme cold conditions in SE Brazil shows the typical characteristics of cold air incursions to the east of the Andes, such as a cold low-level anticyclone over the subtropical continent and a deep cyclonic vortex to the east over the subtropical South Atlantic (Fig. 2). Such conditions result in a northward displacement of the subtropical jet, which leads to a more equator-ward position of the subsiding branch of the Hadley circulation (Vera and Vigliarolo, 2000). This enhancement in the extratropical circulation is also responsible for a significant fraction of the precipitation accumulated during winter and early spring, mostly associated with the passage of extratropical cyclones along the subtropical Atlantic coast (Vera et al., 2001).

Although this extratropical influence persists throughout the year (Garreaud and Wallace, 1998), rainfall during late spring and summer is linked to northerly low-level moisture advection from the Amazon basin related to the

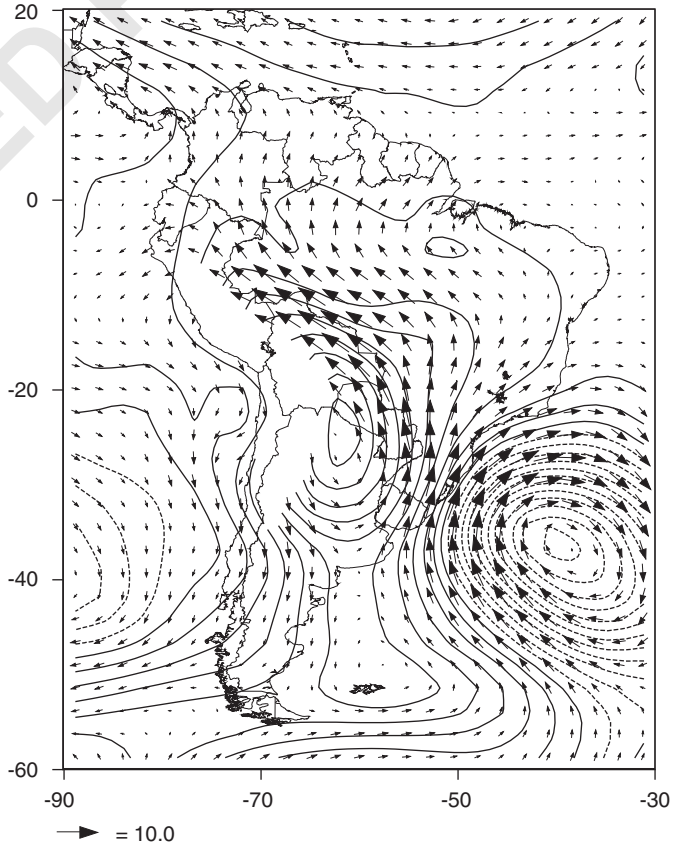

Fig. 2. (a) Composite 850 hPa geopotential height (H_{850}) and wind (u_{850}, v_{850}) during cold episodes in SE Brazil (27.5°S, 50°W) for departure from annual long-term mean minimum temperature. Contour interval is 25 gpm. Gray shading indicates reanalysis topography >1500 m. Scale for wind vector (in m s^{-1}) is shown in lower left.

Table 1
Dating results for speleothem St8

Sample	cm[a]	Wt. (mg)	U (ppm)	^{232}Th (ppm)	^{230}Th/^{232}Th	Measured		Detritus-corrected[b]		Age (10^3 yr)[c]	Initial ^{234}U/^{238}U[d]
						^{230}Th/^{238}U	^{234}U/^{238}U	^{230}Th/^{238}U	^{234}U/^{238}U		
Botuverá Cave/ stalagmite Bt2											
Bt2-3a	1.91	406.75	0.048	0.000485	31.32	0.103±5.006	4.735±0.3	0.102±5.291	4.745±0.319	2.3±0.13	4.770±0.015
Bt2-6a	4.85	411.75	0.068	0.000925	55.33	0.246±0.837	4.281±0.3	0.243±1.037	4.293±0.332	6.3±0.07	4.352±0.014
Bt2-9a	7.73	421.49	0.080	0.001651	55.64	0.379±4.795	4.634±0.17	0.376±4.893	4.654±0.281	9.1± 0.46	4.749±0.014
Bt2-11a	10.31	422.30	0.053	0.000620	117.96	0.453±3.906	4.466±0.325	0.452±3.940	4.472±0.348	11.4±0.47	4.586±0.016
Bt2-12a	11.41	416.05	0.046	0.000774	106.28	0.592±1.631	4.606±0.3	0.591±1.654	4.622±0.351	14.6±0.26	4.775±0.016
Bt2-14a	13.43	420.49	0.038	0.000654	123.87	0.699±3.112	4.331±0.24	0.698±3.136	4.347±0.301	18.6±0.63	4.528±0.015
Bt2-17a	16.15	423.36	0.038	0.000329	293.43	0.836±1.225	4.208±0.3	0.836±1.229	4.218±0.313	23.39±0.32	4.436±0.014
Bt2-19a	18.66	422.81	0.050	0.000705	201.41	0.929±4.406	3.943±0.35	0.929±4.424	3.954±0.379	28.17±1.38	4.12±0.012
Bt2-21a	21.11	421.24	0.050	0.000522	247.77	0.860±1.320	3.280±0.31	0.860±1.325	3.287±0.326	31.83±0.489	3.503±0.011
Bt2-23a	23.60	422.29	0.040	0.000940	153.82	1.180±3.726	3.832±0.274	1.181±3.747	3.850±0.363	38.06±1.64	4.175±0.020
Bt2-25a	28.12	406.45	0.029	0.000156	671.02	1.178±4.008	3.230±0.3	1.178±4.013	3.233±0.304	46.65±2.23	3.549±0.019
Bt2-27a	31.83	421.66	0.041	0.000273	659.00	1.459±1.122	3.165±0.562	1.460±1.124	3.169±0.566	62.2±0.99	3.587±0.019
Bt2-30a	35.62	419.17	0.027	0.000247	557.37	1.681±0.806	3.424±0.31	1.683±0.809	3.430±0.323	67.21±0.75	3.940±0.012
Bt2-32a	38.65	422.35	0.036	0.000594	379.69	2.060±1.218	3.839±0.27	2.065±1.226	3.852±0.318	75.15±1.24	4.528±0.017
Bt2-34a	42.12	424.49	0.044	0.000331	841.73	2.088±1.122	3.714±0.381	2.091±1.124	3.720±0.389	80.09±1.28	4.413±0.018
Bt2-36a	45.63	420.58	0.049	0.000447	759.79	2.285±1.344	3.967±1.02	2.288±1.34	3.973±1.025	82.59±1.91	4.757±0.042
Bt2-40a	55.12	421.50	0.026	0.000406	450.15	2.277±1.713	3.640±0.92	2.282±1.720	3.651±0.934	92.79±2.57	4.448±0.039
Bt2-42b	60.82	420.00	0.049	0.00038	884.2	2.259±1.428	3.348±0.47	2.263±1.431	3.366±0.368	103.8±2.3	4.173±0.022
Bt2-44a	65.30	422.29	0.040	0.000485	587.54	2.358±0.931	3.352±0.891	2.362±0.938	3.359±0.900	110.67±2.21	4.229±0.031
Bt2-46a	68.66	424.87	0.033	0.000522	427.26	2.246±2.814	3.124±0.49	2.252±2.822	3.133±0.513	114.96±5.1	3.954±0.045

Note: All ratios are activity ratios, and all errors are 2s.
[a]Distance from the top of speleothem.
[b]Corrected for detrital U and Th with ^{232}Th/^{238}U = 1.21±50%, ^{230}Th/^{238}U = 1.0±10%, ^{234}U/^{238}U = 1.0±10% (Zero error correlations).
[c]The age uncertainties are at 95% confidence limits.
[d]Backcalculated from the present day, detritus corrected ^{234}U/^{238}U, and the ^{230}Th/U age.

South American Monsoon system (Zhou and Lau, 1998; Gan et al., 2004). Relatively warm conditions persist during austral summer due to a relaxation of the atmospheric circulation over the region. The lack of strong meridional air mass exchange between tropical and mid-latitudes favors the build-up of strong radiative surface heating that results in a temperature increase and the generation of warm days. Warming over the subtropical interior of the continent in the Chaco region to the east of the Andes also contributes to the significantly reduced land–sea temperature contrast.

3. Methods

Age determinations were carried out at the Berkeley Geochronology Center (USA), using conventional chemical and TIMS techniques. Twenty samples, weighting between 409 and 440 mg were cleaned ultrasonically in alcohol, totally dissolved by attack with concentrated HNO_3 and equilibrated with a ^{236}U-^{233}U-^{229}Th spike. U and Th were separated by ion exchange columns, loaded onto outgassed rhenium filaments, and measured on a VG-Sector 54 mass spectrometer equipped with a high abundance-sensitivity filter and Daly ion counter. Instrumental performance was monitored with frequent analyses of Schwartzwalder Mine secular equilibrium standard (Ludwig et al., 1985). Measured isotope ratios were corrected for minor amounts of initial U and Th using ^{232}Th as an index isotope and assuming a typical silicate composition for the contaminant; i.e., activity ratios of ^{232}Th/^{238}U = 1.21±0.6, ^{230}Th/^{238}U = 1.0±0.1, and ^{234}U/^{238}U = 1.0±0.1. U–Th isotopic data and ages are shown in the Table 1. Ages were calculated using the decay constants of Cheng et al. (2000). Age-errors are 95% confidence limits.

Samples for stable isotopic analyses were taken every 1 mm, which represents an average resolution of ~150 years. Oxygen isotope ratios are expressed in δ notation, the per mil deviation from the VPDB standard. For example for oxygen, $\delta^{18}O = [((^{18}O/^{16}O)\text{sample}/(^{18}O/^{16}O)\text{VPDB}) - 1] \times 1000$. For each measurement, approximately 200 μg of powder was drilled from the sample and analyzed with an on-line, automated, carbonate preparation system linked to a Finnigan Delta XL ratio mass spectrometer at the University of Massachusetts. Reproducibility of standard materials is 0.08‰ for $\delta^{18}O$.

4. Results

The carbon and oxygen isotope time-series of Bt2 stalagmite is presented in Fig. 3. Samples were plotted using a linear interpolation based on 20 U/Th ages. The speleothem appears to have grown continuously, as evidenced by lack of detectable hiatuses. Values for stable isotopes on Bt2 range from –2.84 to –7.2‰ (mean −5.7‰) and from −0.5 to −5.0‰ (mean = −2.91‰) for

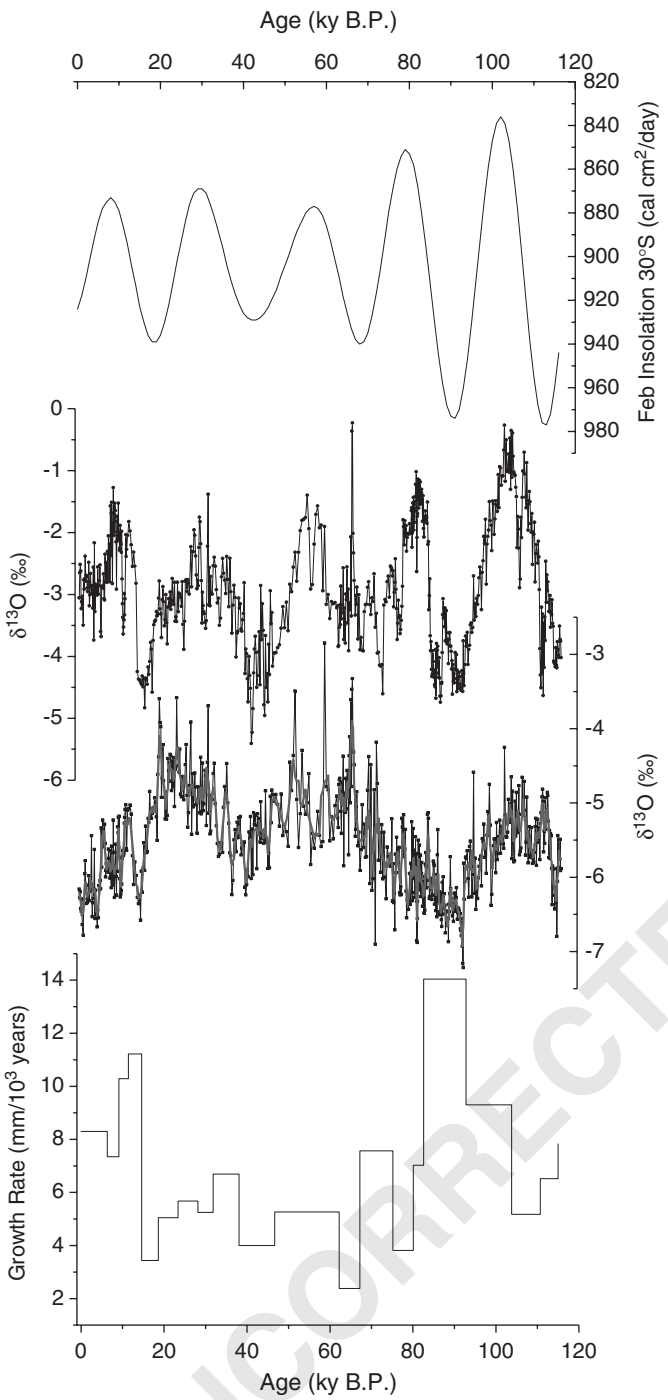

Fig. 3. Stable carbon and oxygen isotope profile for stalagmite BT2. The BT2 profile with a 5pt running average is compared with speleothem growth rates and summer insolation.

$\delta^{13}C$ and $\delta^{18}O$, respectively. They show two distinct behaviors for the last 116,000 years: (i) Relatively rapid $\delta^{13}C$ variations positively covariant with $\delta^{18}O$, from 116 to 108 ky B.P. and after 19 ky B.P.; (ii) More regular changes with predominance of higher values of $\delta^{13}C$ during most parts of the Glacial period from ~75 to 19 ky B.P. and a weakened relationship with $\delta^{18}O$. This trend is interrupted between 107 and 90 ky B.P. by a decrease of ~2.5‰ in the $\delta^{13}C$ values but changes are more gradual than those observed in the oxygen isotope curve. The period from 71 to 19 ky B.P is marked by more attenuated variations and more enriched values of $\delta^{13}C$ (mean = −5.02‰), excepted for the period between 45 and 36 ky B.P., when a slight decrease of ~1‰ in $\delta^{13}C$ is observed. The $\delta^{13}C$ values are marked by an increasing trend from 32 to 19 ky B.P. around the last glacial maximum (LGM) that culminate in values as high as −3.6‰ at 19 ky B.P.

After 19 ky B.P., during deglaciation, there is a substantial decrease in $\delta^{13}C$ with values predominantly lower than the mean value. At this period the $\delta^{13}C$ broadly follows the abrupt variations of $\delta^{18}O$ by showing a positive although lagged covariance relative to the oxygen ratios (Fig. 3). More negative values are observed between 16 and 13 ky B.P. and also after 5 ky B.P. during the middle and late Holocene. Less negative but still lower values than recorded during glacial times occurred from the end of the Pleistocene to the mid-Holocene, between 13 and 5 ky B.P. In addition, the lowest values of $\delta^{13}C$ are coincident with the highest growth rates from 93 to 80 ky B.P. and for the last 15 ky B.P, that range from 9 to 14 mm/10^3years and from 7.4 to 11.2 mm/10^3years, respectively (Fig. 3). These values are significantly higher than mean growth rate observed during most of last glaciation, when values are lower than 7.5 mm/10^3years (mean = 5.1 mm/10^3years).

Spectral analyses show that, unlike $\delta^{18}O$ (Cruz et al., 2005), the $\delta^{13}C$ values of stalagmite Bt2 show no well-defined cyclicity of ~23 ky during the full glacial times (Fig. 3). The $\delta^{13}C$ variations correlate with the summer insolation precession curve during certain time intervals only, as seen at 116–90 ky B.P. and after 19 ky B.P. The dominant cycle in the $\delta^{13}C$ record is 41 ky, a periodicity that has not been commonly reported at relatively low latitude sites (the scale for insolation is reversed in Fig. 7). This cyclicity is confirmed by spectral analysis of the entire $\delta^{13}C$ record, which shows a dominant peak in spectral power at 39 ky, very close to that observed in obliquity (Fig. 4). A striking feature of the breaks in the carbon isotope depletion trend at 91 and 40 ky B.P. is the approximate correspondence with maxima in obliquity (41 ky periodicity) bands, as also observed in the deuterium excess record from the Vostok ice core in East Antarctica (Fig. 7, Vimeux et al., 1999).

5. Discussion

5.1. Paleoclimate inferences from $\delta^{13}C$ and growth rates in Bt2 speleothem

Stalagmite Bt2 appears to have been deposited in approximate isotopic equilibrium with cave drip water as indicated by the absence of a significant correlation between $\delta^{18}O$ and $\delta^{13}C$. This notion is also supported by visible discrepancies between stable isotope variability, as described above, and also by the difference in the relative timing of major changes in $\delta^{13}C$ as compared to $\delta^{18}O$

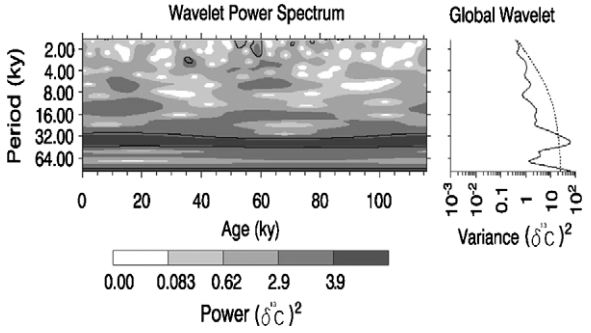

Fig. 4. Spectral analysis of the BT2 $\delta^{13}C$ time series. Left-hand figure is a color-contoured wavelet Morlet analysis of spectral power (interpolated data set has 100 years resolution; 1151 data points), with *y*-axis the Fourier period (in ky B.P.) and the bottom axis age (in ky B.P.). The black contours enclose regions of greater than 95% confidence above a red-noise process. Spectral power is highest at a period of ~39 ky throughout the time series. (b) Right-hand figure is the global wavelet power spectrum (black line). The dashed line is the 95% significance level for a red-noise background. The center of the highest peak above the red noise is at a period of 39 ky.

during the time intervals 116–107 ky B.P., 47–36 ky B.P. and after 20-9 ky B.P (Fig. 3). The estimated average time lag of each mentioned interval, determined by cross-correlation analysis ($\alpha = 0.05$), are 100, 1200 and 900 years, respectively (Fig. 6). Especially during the transition from the last glaciation to the Holocene, the most negative values and the abrupt increase in $\delta^{18}O$ at 15.9 and at 13.8 ky B.P. are recorded in the $\delta^{13}C$ record at 14.7 and at 12.8 ky B.P., respectively. These changes are coincident with the northern hemisphere events Heinrich event H_1 (Broecker and Hemming, 2001) and the Allerod period (Grootes et al., 1993), respectively.

Plausible factors driving the carbon isotope composition of speleothems are changes in the intensity of bedrock limestone dissolution and the carbon isotope composition of CO_2 from sources in soil and atmosphere (Hendy, 1971; Genty et al., 2001a). The relationship between carbon source type and paleoenvironmental processes can be constrained by the Bt2 carbon isotope composition because it was deposited in approximate isotopic equilibrium, as described above. Carbon isotope fractionation resulting from degassing during prior calcite precipitation along the percolation water path above the cave (Baker et al., 1997) can be ruled out as a major factor for $\delta^{13}C$ variations, because $\delta^{13}C$ shows a general anticorrelation with Mg/Ca concentrations in Bt2 (Cruz Jr. et al., manuscript in preparation). This is contrary to the expected tendency if this process had affected the carbon composition, because the prior calcite precipitation would imply higher values of Mg/Ca and increasing CO_2 degassing (Fairchild et al., 2000), which in turn could increase the $\delta^{13}C$ in the seepage water and consequently in the speleothem. In addition, the rates of CO_2 degassing by seasonal shifts in cave atmospheric circulation (Spötl et al., 2005) are unlikely to be the dominant factor in Bt2. $\delta^{13}C$ values would follow the same pattern as speleothem growth rates, because CO_2 degassing increases the saturation index of solution promoting faster calcite precipitation and a speleothem more enriched in ^{13}C, opposite to the observed relationship in the Bt2 time-series.

We argue that the most important determinant of Bt2 carbon isotope variations is changes in the amount of CO_2 input to the soil waters. Processes occurring in the soil, such as the rate of biogenic CO_2 supply from root transpiration, rate of organic matter decomposition (Linge et al., 2001; Frappier et al., 2002) and possibly the type of vegetation cover (Dorale et al., 1998; Denniston et al., 1999) may contribute to changing the soil CO_2 concentration and isotopic composition. Greater soil CO_2 production should result in a greater fraction of the carbon ultimately forming Bt2 coming from isotopically depleted soil sources as opposed to relatively enriched limestone source.

The coincidence of more negative $\delta^{13}C$ with high growth rate values, from 93 to 80 ky B.P. and during the last 15 ky B.P. supports this contention. Processes involved in the CO_2 production and cycling in the soil exert important controls on bedrock dissolution, which is commonly the main mechanism forming H_2CO_3 and consequently controlling HCO_3^-–Ca^{2+} concentrations in karst systems and also speleothem growth rates (Kaufmann and Dreybrodt, 2004).

In terms of interpreting the $\delta^{13}C$ record as some climate parameter, the question then becomes what controls soil CO_2 production? Changes in soil CO_2 productivity around Botuverá cave are possibly modulated by environmental factors such as temperature and rainfall amount or by a combination of both. Although rainfall today has an approximately uniform distribution throughout the year, there are seasonal differences in temperature that could define a growing season during the austral summer. The latter could account for a generally negative tendency of $\delta^{13}C$ that follows the climate amelioration during the deglaciation phase, after 16 ky B.P. Changes in temperature can be a major factor affecting growth rates and $\delta^{13}C$ of speleothems because soil respiration rates are significantly increased under warmer conditions (Reardon et al., 1979; Andrews et al., 2000). Furthermore, the dependence of $\delta^{13}C$ variations on changes in temperature may be even greater during glacial periods because the net primary productivity and soil organic matter decomposition are relatively more sensitive to temperature changes under colder conditions (Kirschbaum, 1995). Although there is some evidence of cooler temperatures in southern Brazil, the climate conditions necessary for soil cover development are likely maintained even during Glacial times. For example, there is no regional evidence of land ice cover or glacial sediment deposits. Also, the lack of depositional hiatuses in stalagmite Bt2 suggests that aridity was not prevalent during Late Pleistocene in the cave site. Thus, we think that the contribution of atmospheric ^{13}C caused by a lack of soil was limited.

On the other hand, the substantial decrease in $\delta^{13}C$ from ~7.5 ky B.P. to the present cannot be attributed to rainfall variability because the dominance of rain forests in lowland coastal regions of Southern Brazil after ~7.5 ky B.P. imply no significant seasonal changes in rainfall amount (Behling and Negrelle, 2001). Moreover, the lack of visible depositional hiatuses over the whole record suggests that intense dryness did not prevail in the cave region. Both factors suggest that the impact of rainfall on soil CO_2 productivity and consequently on $\delta^{13}C$ values was minor. However, we cannot completely rule out the influence of rainfall on biological processes in the soil because time intervals with very negative $\delta^{13}C$ values are coincident with periods of increased rainfall due to the South American summer monsoon (SASM), recorded as more negative values of $\delta^{18}O$ in the Bt2 speleothem at 116–113 93–85, 47–40, 17–13.5 and after 6 ky B.P. (Cruz Jr. et al., 2005a). Therefore, we suggest that the enhancement of summer monsoonal circulation can positively impact the soil CO_2 productivity by promoting warmer and wetter summer conditions, but changes in rainfall regimes probably exert a more subdued influence on soil processes than temperature does.

In a number of other studies of speleothem carbon isotope ratios, changes in $\delta^{13}C$ have been attributed to changes in the dominant photosynthetic pathway of plants overlying the cave. In contrast, however, to pollen–speleothems comparisons in paleoclimate studies of the Midwestern USA (Dorale et al., 1992, 1998; Denniston et al., 1999; Baker et al., 2002) the negative shifts of $\delta^{13}C$ seen in our record after 19 ky do not coincide with periods of forest expansion in southern Brazil according to pollen records from both low-land and over the plateaus in southern Brazil (Behling and Negrelle, 2001; Behling, 2002; Behling et al., 2004, 2005). In lowland Brazil the Volta Velha pollen record at 26°04′S (at sea-level) show that tropical rain forests were the predominant vegetation on the coast only after 7,500 years ago. In addition, grasslands were always dominated the environment south of the cave site at the São Francisco de Paula site at 29°35′S. Arboreal pollen makes up a high percentage of the flora only after ~3200 years (Behling et al., 2005). Furthermore, at all sites over Serra Geral plateaus (Behling, 2002; Behling et al., 2004) forest expansion occurred only during the Late Holocene. The lack of correspondence between changes pollen assemblages and speleothem $\delta^{13}C$, suggests that changes in the percentage of C_4 mixed herbaceous and arboreal plants and C3 arboreal plants in the region is not the main factor controlling the $\delta^{13}C$ variations in our speleothem.

Rapid $\delta^{13}C$ changes, coincident with $\delta^{18}O$ shifts from 116 to 107 ky B.P., 45 to 35 ky B.P. and after 18 ky B.P. (Fig. 3), suggest that the $\delta^{13}C$ responds to large-scale atmospheric variations in the same way the $\delta^{18}O$ does (Cruz Jr. et al., 2005a). Therefore, we suggest that more negative and positive values of $\delta^{13}C$ during these time intervals correspond to periods of enhanced summer monsoon and more intense extratropical circulation over subtropical Brazil, respectively. The positive trends in $\delta^{13}C$ values during periods of weakened SASM, for example at 108–97 and 13–10.5 ky B.P., can be explained by the negative impact of atmospheric cooling on biogenic CO_2 supply, produced by enhanced equatorward advection of midlatitude cold and dry air, as a consequence of more frequent and intense cold surges episodes over southern Brazil, as observed in the modern climatology (Garreaud, 2000; Marengo et al., 2000).

Relevant time lags between the $\delta^{13}C$ and $\delta^{18}O$ time series in Bt2 may reflect more gradual responses of biological activity in soil to changes in climate, which is attributed to the time involved to decompose organic debris into soil (Genty and Massault, 1999; Genty et al., 2003). Contrary to the $\delta^{13}C$, the $\delta^{18}O$ variations of speleothems are considered to be synchronous to the changes in atmospheric circulation patterns in subtropical Brazil because the variations of rainwater isotopic composition can be rapidly transmitted to the speleothems, even in caves with a relatively thick unsaturated zone (Cruz Jr. et al., 2005b). Similar asynchronies, characterized by a time-delay in vegetation shifts relative to abrupt climate change during the late Pleistocene, have been reported in recent studies from tropical South America (Hughen et al., 2004; Jennerjahn et al., 2004). Hence it is important to consider potential differences in response time between proxies when interpreting millennial-scale events based on biological markers.

The soil organic matter decomposition rate appears to have been rather low during most of the last glaciation, as suggested by the general persistence of higher $\delta^{13}C$ values from ~70 to 19 ky B.P. This is the case even in periods of an increased fraction of monsoon rainfall, when $\delta^{18}O$ values are more negative, for example at 78–60 ky B.P., or at 28–19 ky B.P. (Fig. 3). In addition, the $\delta^{13}C$ is increasing while $\delta^{18}O$ remains more negative between 78 and 60 ky B.P. During the second interval, 28–19 ky B.P., on the other hand, $\delta^{13}C$ and $\delta^{18}O$ show synchronous changes, but with opposite signs. A general tendency toward enrichment in ^{13}C can be caused by reduced replenishment of bulk soil organic matter and due to preferential use of ^{12}C during decomposition in the remaining soil by microbes (Nadelhoffer and Fry, 1988). On the basis of the relatively high values of $\delta^{13}C$ between ~70 and 19 ky B.P, we hypothesize that regional cool temperatures kept soil respiration rates low even though $\delta^{18}O$ values suggest a dominantly tropical air mass source for precipitation. Hence, the full glacial conditions in southern Brazil are best represented from ~70 to 19 ky B.P. by the positive $\delta^{13}C$ plateau together with the lowest growth rates in Bt2 (Fig. 3).

This glacial time interval, enriched in ^{13}C, is consistent with glacial boundary conditions as represented by the long-term global cooling from 65 to 18 ky B.P. suggested from deuterium of Vostok (Fig. 5) and with the increase in ice volume during last last glaciation (Martinson et al., 1987; Lambeck and Chappell, 2001). Furthermore, the

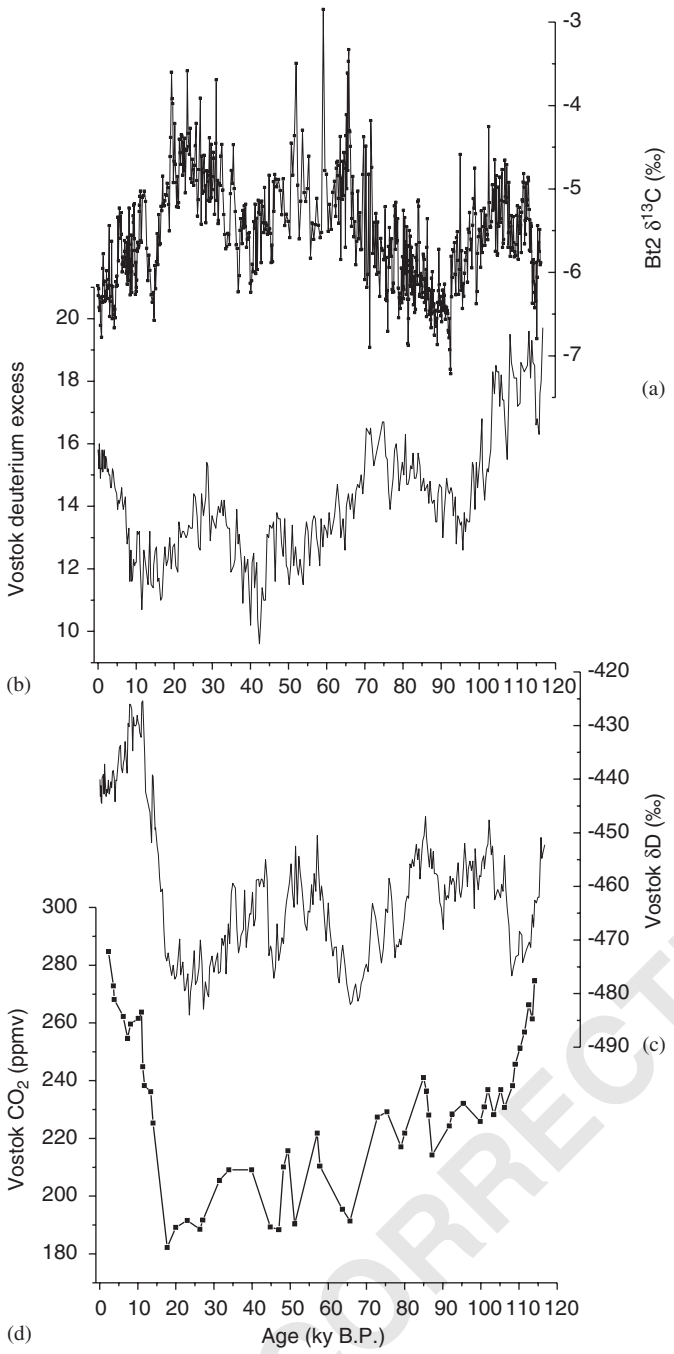

Fig. 5. Comparison between the Bt2 carbon and oxygen isotope time series (a) with CO_2 from Vostok (Petit et al., 1999), Byrd (Neftel et al., 1988) and Taylor Dome Ice-cores (Indermuhle et al., 1999) in Antarctica; (b–c) Deuterium-excess (Vimeux et al., 1999) and δD (Petit et al., 1999) from Vostok Ice core; (d–e) Obliquity and February insolation at 30ϱS (Berger and Loutre, 1991).

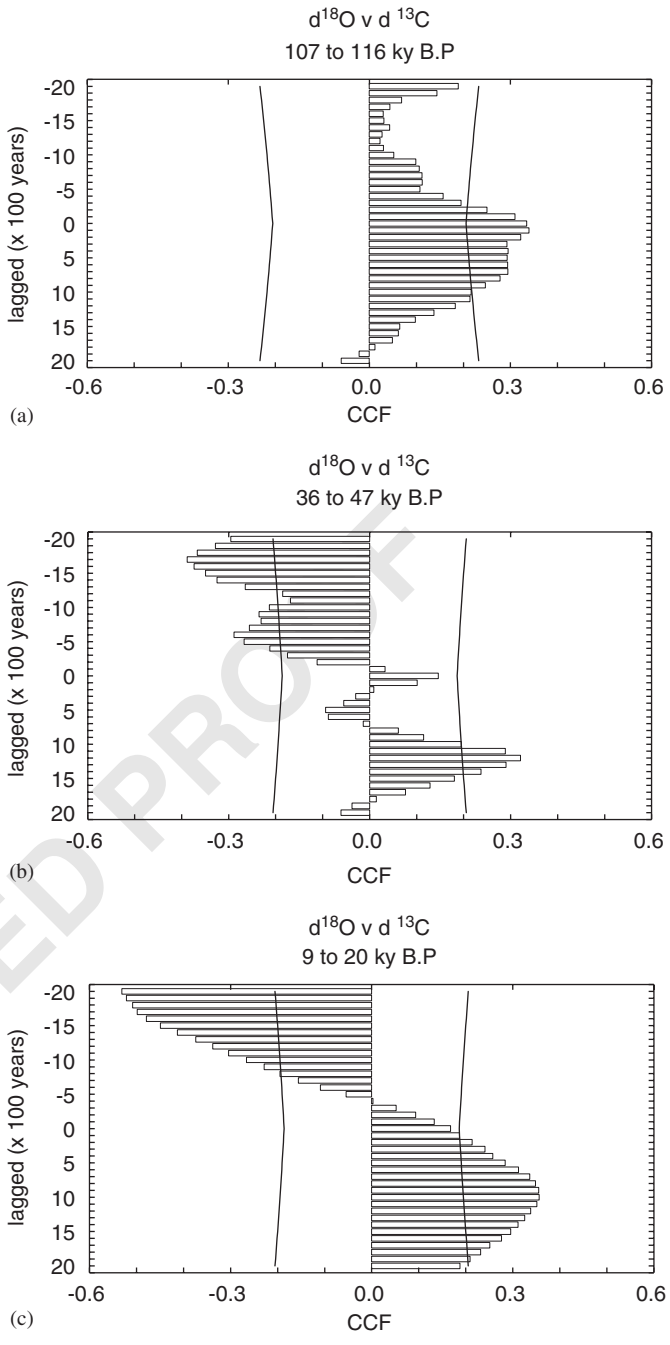

Fig. 6. Cross correlation graphics of stable isotope data for $\delta^{13}C$ and $\delta^{18}O$ at time intervals (a) 20–9 ky B.P., (b) 46–36 ky B.P. and (c) 116–107 ky B.P. The black line represents the confidence level of 95% for analysis. The estimated average time lags of intervals ($\alpha = 0.05$) are 100, 1200 and 900 years, respectively.

significant increase in $\delta^{13}C$ from 35 ky B.P. toward the LGM is consistent with ice sheet growth reported by Winograd (2001). We suggest that the end of the $\delta^{13}C$ increase at ~19 ky B.P. marks the abrupt transition from glacial cooling to warmer conditions during the deglaciation period in subtropical Brazil. The termination of glacial conditions, as constrained here by $\delta^{13}C$ variations, is similar to findings from sites in the tropical Andes (Seltzer et al., 2002; Bush et al., 2004).

The fact that the positive $\delta^{13}C$ plateau in the Bt2 stalagmite between ~70 to 19 ky B.P. matches well the lowest CO_2 concentrations in the Vostok ice core (Fig. 5, Petit et al., 1999), suggests a physical linkage between the isotopic composition of soil CO_2 and the global atmospheric CO_2 concentration during glacial times. A similar connection has previously been established based on

carbon isotope studies in bulk organic matter from lake sediments in Africa (Street-Perrott et al., 1997). Moreover, this pattern agrees with model simulations of terrestrial carbon storage, suggesting that during the LGM only half of today's carbon was stored in the Amazon Basin and surrounding areas due to the impact of large-scale cooling and lower atmospheric CO_2 on the terrestrial biosphere (Mayle and Beerling, 2004).

5.2. Obliquity forcing of climate changes

The absence of a dominant precessional signal in the Bt2 $\delta^{13}C$ record suggests that variations in temperature are to some degree independent of changes in rainfall regimes, as inferred for southern Brazil based on the $\delta^{18}O$ record (Cruz Jr. et al., 2005a). A very strong precession signal at ~23 ky is observed not only in the $\delta^{18}O$ of Bt2 but also in other continental precipitation records from South America (Baker et al., 2001; Stuut and Lamy, 2004). The lack of a precession signal in parts of the $\delta^{13}C$ record (Fig. 3) may be due to persistent cooling during much of the last glacial phase, most evident around the LGM. Temperature variation in subtropical Brazil is related to large-scale pressure patterns and gradients. As a rule, tropical–extratropical atmospheric interactions and associated meridional heat transports depend primarily on the latitudinal temperature gradient, with a stronger gradient leading to increased eddy and total atmospheric energy transport (Rind, 2000).

Lower temperatures in southern Brazil during the past may therefore be a reflection of an enhanced latitudinal temperature gradient, as such conditions would promote an intensification and equatorward shift of the subtropical jet, which in turn would significantly enhance the frequency and intensity of cold surges over the South American subtropics. These colder periods, as inferred by the more negative values of $\delta^{13}C$ during the last glaciation, are broadly consistent with the observed increase in deuterium excess in the Vostok ice core record (Vimeux et al., 1999). The coherence between the d-excess record from Vostok and the carbon isotopes ratios of Bt2 (Fig. 5) can be explained by the fact that both water vapor transport toward Antarctica and changes in temperature over the Brazilian subtropics are strongly influenced by meridional shifts of the atmospheric circulation over the southern hemisphere. Important is the dominance of obliquity in both records, suggesting an increase or decrease of the meridional air mass exchange between the tropics and the extratropics, approximately coincident with maximum and minimum values of obliquity, respectively (Fig. 7).

Raymo and Nisancioglu (2003) in their "Gradient Hypothesis" proposed that the dominance of the obliquity signal on the waxing and waning of ice-sheets during the Pliocene and early Pleistocene is due to its control on meridional temperature gradients. Low obliquity could cause cooling at high latitudes and an increase in the gradient of solar heating between high and low latitudes,

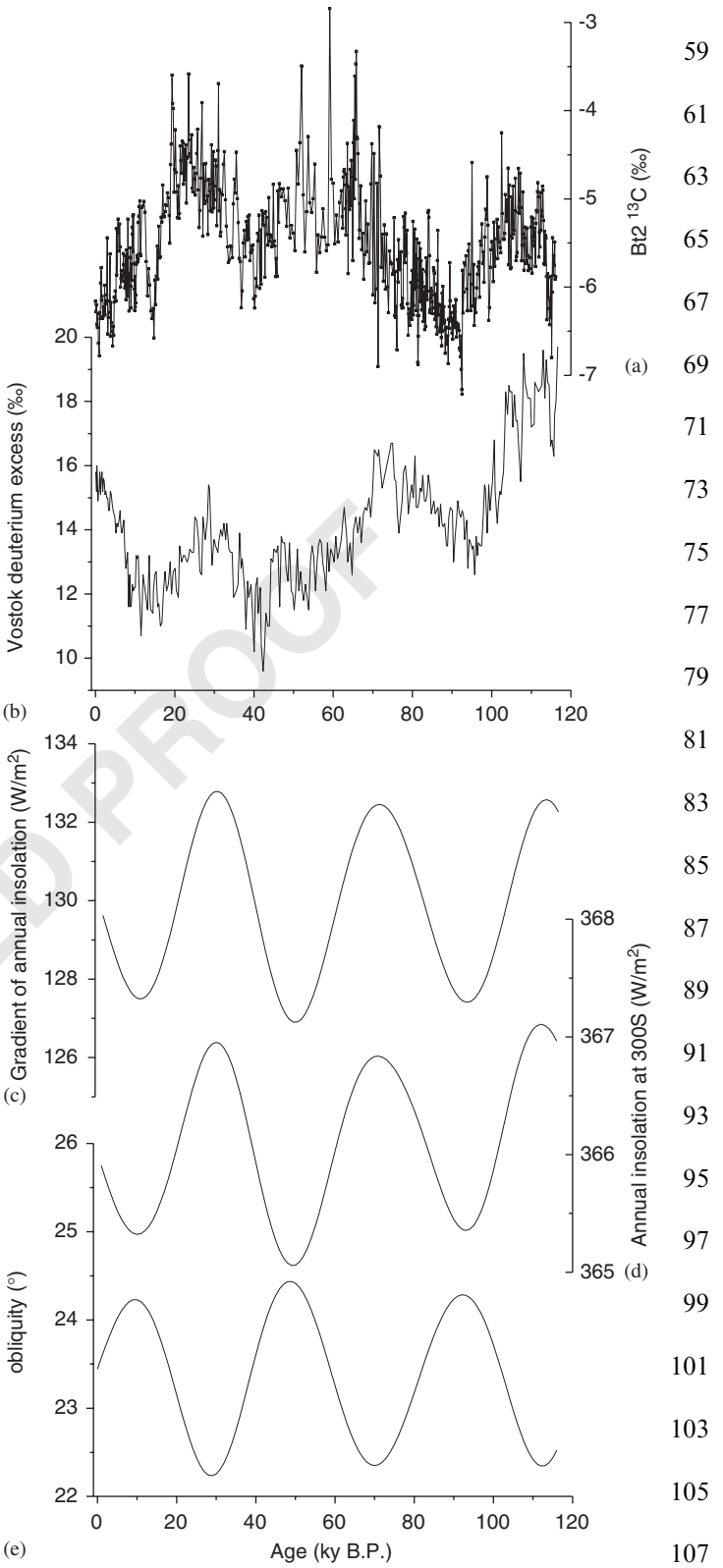

Fig. 7. Comparison between the Bt2 carbon isotope time series (a) with (b) Vostok deuterium excess (Vimeaux et al., 1999), (b) Gradient in annual mean insolation (Loutre et al., 2004), (c) Annual mean insolation at 30°S (Loutre et al., 2004), (d) Obliquity (Berger and Loutre, 1991).

which would enhance the poleward flux of moisture and thus lead to ice sheet expansion in subpolar regions. This mechanism, also used to explain the deuterium excess in Vostok (Vimeux, 1999), was associated with latitudinal differences in annual insolation, which vary essentially with obliquity and do not depend on precession, no matter at what latitude (Loutre et al., 2004). Periods of maximum gradients in annual insolation can only be explained by a rise in the annual mean insolation at low latitudes, since they correspond to phases of lowest annual insolation at high latitudes (Fig. 7). It could be argued that a maximum annual insolation should lead to an increase in radiative heating and thus to higher absolute temperatures over both continent and ocean at low latitudes, which in turn should influence the meridional temperature gradient. However, neither our results nor other tropical continental records from South America (Colinvaux et al., 1996; Bush et al., 2004) or sea surface temperature records at low (Arz, 1998; Martýnez et al., 2003) and at midlatitudes (Lamy et al., 2004) show a warming tendency that would support such a change in the meridional temperature gradient between tropics and subtropics forced by gradient of insolation, at least not around the LGM from 35 to 25 ky B.P. An alternative explanation for such an increased temperature gradient during this period is more intense cooling at high rather than at low latitudes. This cooling could be triggered by lower annual insolation at latitudes higher than 60° in both hemispheres, rather than by the higher annual insolation in the tropics, as proposed by Loutre et al. (2004).

6. Conclusions

Stable isotope variations of carbon and oxygen in the Bt2 stalagmite reveal that shifts between summer monsoonal and winter extratropical circulation patterns can impact local temperature and, consequently, the biological activity in soils. The response of the biological processes, however, can lag behind the climate forcing by several hundred years. These differences in relative timing among carbon and oxygen isotopes highlight the need for multiproxy studies, including independent proxies of atmospheric circulation, to decipher the responses of terrestrial biomarker records to climatic conditions on millennial time-scales.

The predominance of higher $\delta^{13}C$ throughout much of the record from 116 to 19 ky B.P. suggest a significant cooling in southern Brazil due to more frequent, intense and persistent polar cold air incursions over the southern hemisphere subtropics. We argue that the enhancement in extratropical circulation recorded by $\delta^{13}C$ variations during most of the last glacial period, as well as the negative tendency during last glacial times at ~90 and ~40 ky B.P. are probably associated with higher and lower latitudinal temperature gradients, respectively. The strong obliquity signal observed throughout the entire $\delta^{13}C$ time series of Bt2 can be linked to the influence of obliquity on temperature gradients between low and high latitudes; that is, low obliquity values correspond to high temperature gradients, and vice-versa. Furthermore, our results suggest that such enhanced gradients primarily reflect lower temperatures at high latitudes.

7. Uncited References

Chiang et al., 2003; Genty and Massault, 1997; Imbrie et al., 1992; Leuenberger et al., 1992; Musgrove et al., 2001; Rusticucci and Kousky, 2002; Stocker, 1998; Stute et al., 1995.

Acknowledgements

We thank the Fundação de Amparo a Pesquisa do Estado de São Paulo (FAPESP), Brazil, for financial support of this research (Grant 99/10351-6 to I. Karmann and scholarship to F.W. Cruz Jr.). We thank the speleological association GEEP-Açungui and Botuverá's cave guides for supporting field work at Botuverá cave. We are grateful to Dra. Françoise Vimeux for providing the deuterium excess data set of Vostok ice core, annual insolation, gradient of insolation and for fruitful discussions. We very much appreciate the comments by Dr. Andy Baker and an anonymous referee.

References

Arz, H., 1998. Dokumentation von kurzfristigen Klimaschwankungen des Spätquartärs in Sedimenten des westlichen äquatorialen Atlantiks. Berichte, Fachbereich Geowissenschaften, Universität Bremen 124, 96pp.

Amundson, R., Stern, L., Baisden, T., Wang, Y., 1998. The isotopic composition of soil and soil-respired CO_2. Geoderma 82, 83–114.

Andrews, J.A., Matemala, R., Westover, K.M., Schlesinger, W.H., 2000. Temperature effects on the diversity of soil heterotrophs and $\delta^{13}C$ of soil-respired. Soil Biology and Biochemistry 32, 699–706.

Baker, A., Ito, E., Smart, P.L., McEwan, R.F., 1997. Elevated and variable values of $\delta^{13}C$ in speleothems in a British cave system. Chemical Geology 136, 263–270.

Baker, A., Genty, D., Dreybrodt, Barnes, W.L., Mockler, N., Grapes, J., 1998. Testing theoretically predicted stalagmite growth rate with recent annually laminated samples: implication for past stalagmite deposition. Geochimica et Cosmochimica Acta 62 (3), 393–404.

Baker, P.A., Rigsby, C.A., Seltzer, G.O., Fritz, S.C., Lowenstein, T.K.K., Bacher, N.P., Veliz, C., 2001. Tropical climate changes at millennial and orbital timescales on the Bolivian Altiplano. Nature 409, 698–700.

Baker, R.G., Bettis III, E.A., Denniston, R.F., Gonzalez, L.A., Strickland, L.E., Krieg, J.R., 2002. Holocene paleoenvironments in southeastern Minnesota chasing the prairie-forest ecotone. Palaeogeography, Palaeoclimatology, Palaeoecology 177, 103–122.

Baldini, J.U.L., McDermott, F., Fairchild, I.J., 2002. Structure of the 8200 year cold event revealed by a speleothem trace element record. Science 296, 2203–2206.

Baldini, J.U.L., McDermott, F., Baker, A., Baldini, L.M., Mattey, D.P., Railsback, L.B., 2005. Biomass effects on stalagmite growth and isotope ratios: A 20th century analogue from Wiltshire, England. Earth and Planetary Science Letters 240, 486–494.

Behling, H., 2002. South and Southeast Brazilian grasslands during Late Quaternary times: a synthesis. Palaeogeography, Palaeoclimatology, Palaeoecology 177, 19–27.

Behling, H., Negrelle, R.R.B., 2001. Tropical rain forest and climate dynamics of the Atlantic lowland, Southern Brazil, during the Late Quaternary. Quaternary Research 56, 383–389.

Behling, H., Pillar, V.D., Orlóci, L., Bauermann, S.G., 2004. Late Quaternary araucaria forest, grassland (campos), fire and climate dynamics, studied by high-resolution pollen, charcoal and multivariate analysis of the Cambará do Sul core in southern Brazil. Palaeogeography, Palaeoclimatology, Palaeoecology 203, 277–297.

Behling, H., Pillar, V.D., Bauermann, S.G., 2005. Late Quaternary grassland (Campos), gallery forest, fire and climate dynamics, studied by pollen, charcoal and multivariate analysis of the São Francisco de Assis core in western Rio Grande do Sul (southern Brazil). Review of Palaeobotany and Palynology 133, 235–248.

Berger, A., Loutre, M.F., 1991. Insolation values for the climate of the last 10 million years. Quaternary Science Reviews 10, 297–317.

Broecker, W.S., Hemming, S., 2001. Climate swings come into focus. Science 294, 2308–2309.

Bush, M.B., Silman, M.R., Urrego, D.H., 2004. 48,000 Years of climate and forest change in a biodiversity hot spot. Science 303, 827–829.

Campanha, G.C., Sadowski, G.R., 1999. Tectonics of the southern portion of Ribeira Belt (Apiaí Domain). Precambian Research 98, 31–51.

Charman, D.J., Caseldine, C., Baker, A., Gearey, B., Hatton, J., Proctor, C., 2001. Paleohydrological records from peat profiles and speleothems in Sutherland, Northwest Scotland. Quaternary Research 55, 223–234.

Cheng, H., Edwards, R.L., Hoff, J., Gallup, C.D., Richards, D.A., Asmerom, Y., 2000. The half-lives of uranium-234 and thorium-230. Chemical Geology 169, 17–33.

Chiang, J.C.H., Biasutti, M., Battisti, D.S., 2003. Sensitivity of the Atlantic Intertropical Convergence Zone to the last glacial maximum boundary conditions. Paleoceanography 18 (4).

Colinvaux, P., De Oliveira, P.E., Moreno, J.E., Miller, M.C., Bush, M.B., 1996. A long pollen record from lowland Amazonia: Forest and cooling in glacial times. Science 274, 85–88.

Cruz Jr., F.W., Burns, S.J., Karmann, I., Sharp, W.D., Vuille, M., Cardoso, A.O., Ferrari, J.A., Silva Dias, P.L., Viana Jr., O., 2005a. Insolation-driven changes in atmospheric circulation over the past 116 ky in subtropical Brazil. Nature 434, 63–66.

Cruz Jr., F.W., Karmann, I., Viana Jr., O., Burns, S.J., Ferrari, J.A., Vuille, M., Moreira, M.Z., Sial, A.N., 2005b. Stable isotope study of cave percolation waters in subtropical Brazil: implications for paleoclimate inferences from speleothems. Chemical Geology 220, 245–262.

Denniston, R.F., González, L.A., Baker, R.G., Asmerom, Y., Reagan, M.K., Edwards, R.L., Alexander, E.C., 1999. Speleothem evidence for Holocene fluctuations of the prairie-forest ecotone, north-central USA. The Holocene 9, 671–676.

Desmarchelier, J.M., Goede, A., Ayliffe, L.K., McCulloch, M.T., Moriarty, K., 2000. Stable isotope record and its palaeoenvironmental interpretation for a late Middle Pleistocene speleothem from Victoria Fossil Cave, Naracoorte, South Australia. Quaternary Science Reviews 19, 763–774.

Dorale, J.A., González, L.A., Reagan, M.K., Pickett, D.A., Murrell, M.T., Baker, R.G., 1992. A high resolution record of Holocene climate change in speleothem calcite from Cold Water Cave, northeast Iowa. Science 258, 1626–1630.

Dorale, J.A., Edwards, R.L., Ito, E., González, L.A., 1998. Climate and vegetation history of the midcontinent from 75 to 25 ka: A speleothem record from Crevice Cave, Missouri, USA. Science 282, 1871–1874.

Drysdale, R.N., Zanchetta, G., Hellstrom, J.C., Fallick, A.E., Zhao, J.X., Isola, I., Bruschi, G., 2004. Palaeoclimatic implications of the growth history and stable isotope ($\delta^{18}O$ and $\delta^{13}C$) geochemistry of a Middle to Late Pleistocene stalagmite from central-western Italy. Earth and Planetary Science Letters 227, 215–229.

Dulinski, M., Rozanski, K., 1990. Formation of 13C/12C isotope ratios in speleothems: a semi-dynamic model. Radiocarbon 32, 7–16.

Fairchild, I.J., Borsato, A., Tooth, A.F., Frisia, S., Hawkeswirth, C.J., Huang, Y., McDermot, F., Spiro, B., 2000. Controls on trace element (Sr–Mg) compositions of carbonate cave waters: implications for speleothem climatic records. Chemical Geology 166, 255–269.

Frappier, A., Sahagian, D., González, L., Carpenter, S.J., 2002. El Ninõ Events Recorded by Stalagmite Carbon Isotopes. Science 298, 565.

Frumkim, A., Ford, D.C., Schwarcz, H.P., 2000. Paleoclimate and vegetation of the last glacial cycles in Jerusalem from a speleothem record. Global Biogeochemical Cycles 14 (3), 863–870.

Gan, M.A., Kousky, V.E., Ropelewski, C.F., 2004. The South American monsoon circulation and its relationship to rainfall over West-Central Brazil. Journal of Climate 17, 47–66.

Garreaud, R.D., Wallace, J., 1998. Summertime incursions of midlatitude air into subtropical and tropical South America. Monthly Weather Review 126, 2713–2733.

Garreaud, R.D., 1999. Cold air incursions over subtropical and tropical South America: A numerical case study. Monthly Weather Review 127, 2823–2853.

Garreaud, R.D., 2000. Cold air incursions over subtropical South America: mean structure and dynamics. Monthly Weather Review 128, 2544–2559.

Gascoyne, M., 1992. Palaeoclimate determination from cave calcite deposits. Quaternary Science Reviews 11, 609–632.

Genty, D., Massault, M., 1997. Carbon transfer dynamics from bomb C-14 and delta C-13 time series of a laminated stalagmite from SW France modelling and comparison with other stalagmite records. Geochimica et Cosmochimica Acta 63, 1537–1548.

Genty, D., Baker, A., Massault, M., Proctor, C., Gilmour, M., Pons-Branchu, E., Hamelin, B., 2001a. Dead carbon in stalagmites: carbonate bedrock paleodissolution vs. ageing of soil organic matter: Implications for ^{13}C variations in speleothems. Geochimica et Cosmochimica Acta 65, 3443–3457.

Genty, D., Baker, A., Vokal, B., 2001b. Intra and inter-annual growth rate of modern stalagmites. Chemical Geology 176, 191–212.

Grootes, P.M., Stuiver, M., White, J.W.C., Johnsen, S., Jouzel, J., 1993. Comparison of oxygen isotopes records from the GISP2 and GRIP Greenland ice cores. Nature 366, 552–554.

Hendy, C.H., 1971. The isotopic geochemistry of speleothems-I. The calculation of the effects of different modes of formation on the isotopic composition of speleothems and their applicability as paleoclimatic indicators. Geochimica et Cosmochimica Acta 35, 801–824.

Hesterberg, R., Siegenthaler, U., 1991. Production and stable isotopic composition of CO_2 in a soil near Bern, Switzerland. Tellus 43B, 197–205.

Hughen, K.A., Eglinton, T.I., Xu, L., Makou, M., 2004. Abrupt tropical vegetation response to rapid climate changes. Science 304, 1955–1958.

Imbrie, J., et al., 1992. On the structure and origin of major glaciation cycles, 1, Linear responses to Milankovitch forcing. Paleoceanography (7), 701–738.

Jennerjahn, T.C., Venugopalan, I., Arz, H.W., Behling, H., Patzold, J., Wefer, G., 2004. Asynchronous terrestrial and marine signals of climate change during Heinrich events. Science 306, 2236–2239.

Kalnay, E., Kanamitsu, M., Kistler, R., Collins, W., Deaven, D., Gandin, L., Iredell, M., Saha, S., White, G., Woollen, J., Zhu, Y., Chelliah, M., Ebisuzaki, W., Higgins, W., Janowiak, J., Mo, K.C., Ropelewski, C., Wang, J., Leetmaa, A., Reynolds, R., Jenne, R., Joseph, D., 1996. The NCEP/NCAR 40-year reanalysis project. Bulletin of the American Meteorological Society 77 (3), 437–471.

Kaufmann, G., Dreybrodt, W., 2004. Stalagmite growth and palaeoclimate: an inverse approach. Earth and Planetary Science Letters 224, 529–545.

Kirschbaum, M., 1995. The temperature dependence of soil organic matter decomposition, and the effect of global warming on soil organic C storage. Soil Biology Biochemistry 27 (6), 753–760.

Lamy, F., Kaiser, J., Ninnemann, U., Hebbeln, D., Arz, H.W., Stoner, J., 2004. Antarctic timing of surface water changes off Chile and Patagonian ice sheet response. Science 304, 1959–1962.

Leuenberger, M., Siegenthaler, U., Langway, C.C., 1992. Carbon isotope composition of atmospheric CO2 during the last ice age from an Antarctic ice core. Nature 357, 488–490.

Lambeck, K., Chappell, J., 2001. Sea level change through the last glacial cycle. Science 292, 679–686.

Linge, H., Lauritzen, S.E., Lundberg, J., Berstad, I.M., 2001. Stable isotope stratigraphy of Holocene speleothems: examples from a cave system in Rana, northern Norway. Palaeogeography, Palaeoclimatology, Palaeoecology 167, 209–224.

Ludwig, K.R., Wallace, A.R., Simmons, K.R., 1985. The Schwartzwalder uranium deposit.2. Age of uranium mineralization and lead isotope constraints on genesis. Economic Geology 80 (7), 1858–1871.

Marengo, J.A., Ambrizzi, T., Kiladis, G., Liebmann, B., 2002. Upper-air wave trains over wintertime cold surges in tropical-subtropical South America leading to freezes in Southern and Southeastern Brazil. Theoretical and Applied Climatology 73, 223–242.

Martýnez, I., Keigwin, L., Barrows, T.T., Yokoyama, Y., Southon, J., 2003. La Ninã -like conditions in the eastern equatorial Pacific and a stronger Choco jet in the northern Andes during the last glaciation. Paleoceanography 18 (2).

Martinson, D.G., Pisias, N.G., Hays, J.D., Imbrie, J., Moore, T.C., Shackleton, N.J., 1987. Age dating and the orbital theory of the ice ages: development of a high resolution 0 to 300,000-year chronostratigraphy. Quaternary Research 27, 1–19.

Mayle, F.E., Beerling, D., 2004. Late Quaternary changes in Amazonian ecosystems and their implications for global carbon cycling. Palaeogeography, Palaeoclimatology, Palaeoecology 214, 11–25.

McDermott, F., 2004. Palaeo-climate reconstruction from stable isotope variations in speleothems: a review. Quaternary Science Reviews 23, 901–918.

Musgrove, M., Banner, J.L., Mack, L.E., Combs, D.M., James, E.W., Cheng, H., Edwards, R.L., 2001. Geochronology of late Pleistocene to Holocene speleothems from central Texas: Implications for regional paleoclimate. Geological Society of America Bulletin 113, 1532–1543.

Nadelhoffer, K.F., Fry, B., 1988. Controls on natural nitrogen-15 and carbon-13 abundance in forest soil organic matter. Soil Science Society America of Journal 52, 1633–1640.

Petit, J.-R., Jouzel, J., Raynaud, D., Barkov, N.I., Barnola, J.-M., Basile, I., Bender, M.L., Chappellaz, J., Davis, M.E., Delaygue, G., Delmotte, M., Kotlyakov, V.M., Legrand, M., Lipenkov, V.Y., Lorius, C., Pépin, L., Ritz, C., Saltzman, E., Stievenard, M., 1999. Climate and atmospheric history of the past 420,000 years from the Vostock ice core, Antarctica. Nature 399, 429–436.

Plagnes, V., Causse, C., Genty, D., Paterne, M., Blamart, D., 2002. A discontinuous climatic record from 187 to 74 ka from a speleothem of the Clamouse Cave (south of France). Earth and Planetary Science Letters 201, 87–103.

Polyak, V.J., Rasmussen, J.B.T., Asmerom, Y., 2004. Prolonged wet period in the southwestern United States through the Younger Dryas. Geology 32 (1), 5–8.

Rao, V.B., Hada, K., 1990. Characteristics of rainfall over Brazil: annual variations and connections with the Southern Oscillation. Theoretical and Applied Climatology 42, 81–90.

Rusticucci, M.M., Kousky, V.E., 2002. A comparative study of maximum and minimum temperatures over Argentina: NCEP-NCAR reanalysis versus station data. Journal of Climate 15, 2089–2101.

Raymo, M.E., Nisancioglu, K., 2003. The 41 kyr world: Milankovitch's other unsolved mystery. Paleoceanography 18 (1).

Reardon, E.J., Allison, G.B., Fritz, P., 1979. Seasonal chemical and isotopic variations of soil CO_2 at Trout Creek, Ontario. Journal of Hydrology 43, 355–371.

Seluchi, M.E., Marengo, J.A., 2000. Tropical-midlatitude exchange of air masses during summer and winter in South America: climatic aspects and examples of intense events. International Journal of Climatology 20, 1167–1190.

Seltzer, G.O., Rodbell, D.T., Baker, P.A., Fritz, S.C., Tapia, P.M., Rowe, H.D., Dunbar, R.B., 2002. Early warming of tropical South America at the last glacial–interglacial transition. Science 296, 1685–1686.

Stocker, T.F., 1998. The seesaw effect. Science 282, 61–62.

Street-Perrott, F.A., Huang, Y., Perrott, R.A., Eglinton, G., Barker, P., Ben Khelifa, L., Harkness, D.D., Olago, D.O., 1997. Impact of lower atmospheric carbon dioxide on tropical mountain ecosystems. Science 278, 1422–1426.

Stute, M., Forster, M., Frischkorn, H., Serejo, A., Clark, J.F., Schlosser, P., Broecker, W.S., Bonani, G., 1995. Cooling of tropical Brazil (5 °C) during the Last Glacial Maximum. Science 269, 379–383.

Stuut, J-B.W., Lamy, F., 2004. Climate variability at the southern boundaries of the Namib (southwestern Africa) and Atacama (northern Chile) coastal deserts during the last 120,000 yr. Quaternary Research 62, 301–309.

Vera, C.S., Vigliarolo, P.K., 2000. A diagnostic study of cold-air outbreaks over South America. Monthly Weather Review 128, 3–24.

Vera, C.S., Vigliarolo, P.K., Berbery, E.H., 2002. Cold season synoptic-scale waves over subtropical South America. Monthly Weather Review 130, 684–699.

Vimeux, F., Masson, V., Jouzel, J., Stievenard, M., Petit, J.R., 1999. Glacial–interglacial changes in ocean surface conditions in the southern hemisphere. Nature 398, 410–413.

Williams, P.W., King, D.N.T., Zhao, J.-X., Collerson, K.D., 2005. Late Pleistocene to Holocene composite speleothem 18O and 13C chronologies from South Island, New Zealand—did a global Younger Dryas really exist? Earth and Planetary Science Letters 230, 301–317.

Winograd, I.J., 2001. The magnitude and proximate cause of ice-sheet growth since 35,000 yr B. P. Quaternary Research 56, 299–307.

Zhou, J., Lau, K.M., 1998. Does a Monsoon Climate Exist over South America? Journal of Climate 11, 1020–1040.